20

Mechanics of Cold Rolling of Thin Strip

Z. Y. Jiang
School of Mechanical, Materials and Mechatronic Engineering,
University of Wollongong, Wollongong,
Australia

1. Introduction

Cold rolled thin strip has a wide application in electronic and instrument industries, and its production has always been of major interest to the manufacturers and researchers in the area of metal plasticity. Thin strip rolling involves significant metal plasticity to produce a desired product. Iwamoto (2004), Stoughton & Yoon (2004) and Huh et al. (2004) were interested in dealing with the plastic deformation and plastic yielding of steel, and its micro-mechanics. With the need for higher quality and productivity in cold strip mill, mathematical models of cold rolling of a strip with a desired shape and dimension, both for mill set-up and for on-line control, have become a key issue in the steel rolling process. One major part of these models concerns the strip and roll deformation, plastically deformed strip shape and profile. The development of the roll deformation model can be divided into three groups, which includes simple beam model, slit beam model and finite element analysis model (Ginzburg, 1989). Stone & Gray (1965) modelled the roll deformation as the deflection of a simple beam on an elastic foundation. Shohet & Townsend (1968) proposed a slit beam deflection model, and then Edwards & Spooner (1973), Wang (1986) improved this theory and introduced a matrix method to solve the beam deflection considering strip plastic deformation. It has now been widely used in analysis of the roll deformation and strip shape and profile. Timoshenko & Goodier (1970), Jiang et al. (2003a, b, c), Komori (1998) and Lin & Lee (1997) used finite element model and numerical methods to analyse the strip rolling and to improve the simulation accuracy of the strip shape and profile. In order to improve the quality of the produced products, Kim & Oh (2003) used finite element method to analyse grain-by-grain deformation by crystal plasticity with couple stress, Simth et al. (2003) conducted a study of the effect of the transverse normal stress on sheet metal formability and Ho et al. (2004) developed integrated numerical techniques to predict springback in creep forming thick aluminum sheet components. Buchheit et al. (2005) performed simulations of realistic looking 3-D polycrystalline microstructures generated. The simulation on precipitate induced hardening in crystal plasticity was conducted (Han et al., 2004). Martin & Smith (2005) investigated the influence of the compressive through-thickness normal stress on sheet metal formability and tried to explore the ways to improve the sheet metal formability. However, the finite element analysis is rather complicated and may have a convergence problem, which is difficult to be used for on-line control of the thin strip rolling. An influence function method analysis considering the strip plastic deformation and roll deformation can be directly used in the control of strip rolling, especially in the control of the shape and profile of strip.

In practical rolling of thin strip, there is a phenomenon that the upper and lower work rolls may contact each other beyond the edges of strip if the strip is very thin and there is no work roll bending applied as shown in Fig. 1. m and n are the number of the slab elements along the half roll barrel and half strip width respectively. Δx is the width of each element; D_w the diameter of work roll; D_b the diameter of backup roll; d_w the diameter of work roll neck; d_b the diameter of backup roll neck; L_w the half-width of work roll barrel; L_b the half-width of backup roll barrel; F the bending force; P the rolling force; q_j the intermediate force between the work roll and backup roll at element j; p_j the rolling force at element j; q_{em} the edge contact force between the upper and down work rolls acting on slab element m; B the strip width; L_1 the central distance between the work roll bending cylinders, L_2 the central distance between the housing screws and L_e the roll edge contact length. This case often occurs during the thin strip rolling, and the rolled strip shape and profile will be affected significantly if the control model is not applicable. Roll edge contact force between the upper and down work rolls will change with different rolling conditions. The delivered thickness distribution of strip depends on the material properties, the reduction of plastic deformation, roll thermal and mechanical crown, roll wear profile, the roll deformations due to the deflection of the rolls, the local contact effect which includes the flattening between the work roll and backup roll, the flattening between the work roll and strip and the edge contact of the work rolls. The edge contacts of the work rolls affect the deformation of the rolls and the strip shape, thus forming a new deformation feature including strip plastic deformation and roll deformation in the cold rolling process. In this case, the models of deformation and plasticity are different from the traditional analysis in plasticity in cold strip rolling. Not only will the distribution of the roll pressure change when the work rolls contact beyond the edges of the strip, but also the plastic deformation of strip and the deformation model of work rolls (Edwards & Spooner, 1973, Kuhn & Weinstein, 1970), friction variation at the interface of the rolls and the strip, and work roll wear (Lenard, 1992, 1998, Liu et al., 2001, Jiang & Tieu, 2001). Sutcliffe et al. (1998, 2001) developed a robust model for rolling of thin strip and foil and carried out experimental measurements of load and strip profile. A comparison of roll torque and lateral spread was also conducted for thin strip rolling (Shi et al., 2001). The real contact area is relevant to the contact friction coefficient. Stupkiewicz & Mroz (2003) developed a phenomenological model to calculate the real contact area accounting for bulk plastic deformation in metal forming. How to determine the distribution of rolling force and the strip shape and to find a method to improve its shape and profile when the work rolls contact beyond the strip edges are the main features of this study. The effect of the strip width and transverse friction on the roll edges contact length, the rolling force and strip shape will be quantified and discussed in this study.

In this chapter, a modified semi-infinite body model was introduced to calculate the flattening of work roll/backup roll, work roll/strip, and the Foppl model (Ginzburg & Azzam, 1997) was employed to simulate the edge contact between the upper and down work rolls. Based on the theory of the slit beam, this special cold rolling of thin strip was calculated using an influence function method. The rolling force determined from the plasticity of metal forming was iterated in the simulation, and the analysis of the mechanics of the rolls is for dealing with the plasticity of this special rolling through factors such as the

rolling force and torque, and the strip plastic deformation such as the strip shape and profile. A comparison of the forces and the strip shape with or without the work roll edge contact was carried out. The effects of the different rolling parameters, such as the reduction, strip width, friction coefficient and transverse friction distribution, on the mechanics and deformation of the cold rolling of thin strip were analyzed. The developed model is useful in improving the shape and flatness quality of thin strip in cold rolling process. Based on the developed method and research results, a comprehensive model which is suitable for considering the work roll edge contact or not can be obtained.
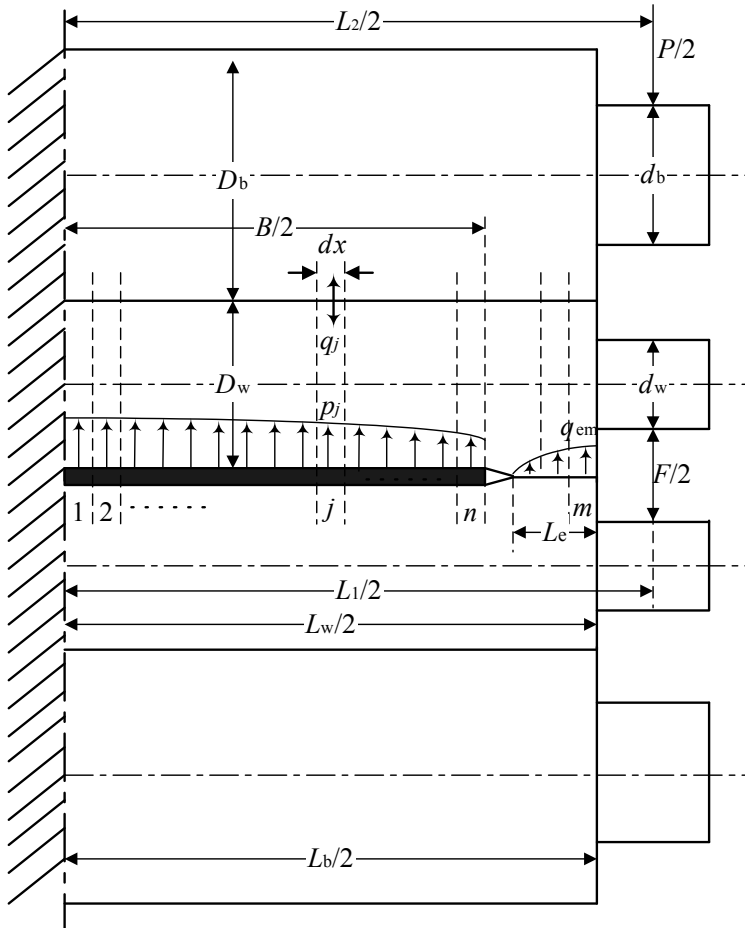
Fig. 1. Edge contact of work rolls and Slit beam deflection mode for a 4-high rolling mill

2. Roll deformation of 4-high rolling mill

As symmetry of the mill about the mid-span of the rolls, the calculation process involves one half of a roll system. Given in Fig. 1, one half of the roll barrel and the strip are divided into

m and n slab elements respectively. The rolling pressure, the pressure between the work roll and backup roll, and that between the upper and down work rolls are uniform in each element, which are replaced by a concentrated load applied to the middle of each element. The profile of the deformed work roll and backup roll are obtained by calculating the roll deflections due to bending and shear forces. Local deformations due to the flattening in the contact region between the work roll and backup roll, between the work roll and strip, and between the upper and down work rolls are added to the roll deflections.

As shown in Fig. 2, if $G(x,x')$ is the deformation of the beam at position x caused by a unit load which is applied to the beam at position x', the deformation of the beam at position x caused by an arbitrary load distribution along the beam can be calculated by the following equation,

$$y(x) = \int G(x,x') \cdot p'(x') dx' \tag{1}$$

where $G(x,x')$ is the influence function in the linear mechanical field. If the load distribution is handled as a number of concentrated loads at the middle of each element, Eq. (1) can be expressed as

$$y(i) = \sum_{j}^{m} g(i,j) p_j \tag{2}$$

where the influence function, $g(i,j)$, is defined as the deflection in the middle of the element i due to a unit load applied to the middle of the element j. The deformation, $y(i)$, in Eq. (2) not only indicates the deflection of the roll, but also represents the flattening of the contact zone.
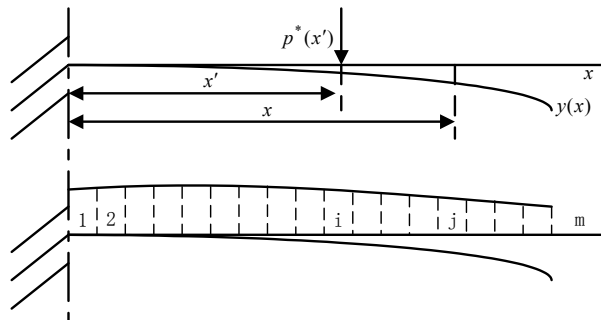

Fig. 2. Deformation of the roll from an arbitrary load distribution

2.1 Deflection of the work rolls

The deflection of the work rolls due to bending and shear forces can be described as the vertical displacement of the work roll at element i by the following equation,

$$y_w(i) = \sum_{j=1}^{m} g_w(i,j) q_j - \sum_{j=1}^{n} g_w(i,j) p_j - \sum_{j=k}^{m} g_w(i,j) q_{ej} - g_{wf}(i) F \tag{3}$$

where $y_w(i)$ is the vertical deflection of the work roll at element i, $g_w(i,j)$ is the influence function for the work roll deflection due to the combined bending and shear forces generated by rolling load, $g_{wf}(i)$ is the influence function for the work roll deflection due to the force generated by the roll bending mechanism, k represents the minimum element number of the edge contact length caused by the flattening between the upper and down work rolls.

The exact forms of the influence functions $g_w(i,j)$ and $g_{wf}(i)$ are described in Reference (Edwards & Spooner, 1973) according to the theorem of Castigliano (Timoshenko & Goodier, 1970), which can be defined as follows

$$g_w(i,j) = \frac{1}{6E_w I_w}(x_j^2(3x_i - x_j) + (1+\nu_w)D_w^2 x_j) \qquad x_i \geq x_j$$
$$= \frac{1}{6E_w I_w}(x_i^2(3x_j - x_i) + (1+\nu_w)D_w^2 x_i) \qquad x_i < x_j \tag{4}$$

$$g_{wf}(i) = \frac{1}{6E_w I_w}(x_i^2(3L_1 - x_i) + (1+\nu_w)x_i D_w^2) \tag{5}$$

where E_w is the work roll modulus of elasticity, ν_w is Poisson's ratio of the work roll and I_w is the moment of inertia of the work roll section.

2.2 Deflection of the backup rolls

The deformation of the backup roll can be expressed as the vertical displacement of the backup roll at the i th element,

$$y_b(i) = \sum_{j=1}^{m} g_b(i,j)q_j \tag{6}$$

where $y_b(i)$ is the vertical deflection of the backup roll at element i, $g_b(i,j)$ is the influence function for the backup roll deflection, which has been derived by Edwards & Spooner (1973)

$$g_b(i,j) = \frac{1}{6E_b I_b}(3x_i^2(L_b - x_j) - (x_i - x_j)^3 + (1+\nu_b)(x_i - x_j)D_b^2) \qquad x_i \geq x_j$$
$$= \frac{1}{6E_b I_b}(3x_i^2(L_2 - x_j)) \qquad x_i < x_j \tag{7}$$

where E_b is the backup roll modulus of elasticity, ν_b is Poisson's ratio of the backup roll and I_b is the moment of inertia of the backup roll section.

2.3 Flattening between the work roll and strip

As shown in Fig. 3, the infinite plane π is the boundary of a semi-infinite body, the upper side of the plane π is the semi-infinite space and the down side is the semi-infinite solid. When a force P acts on this plane at position O, the vertical displacement at point B produced by the force P is as follows

$$w = \frac{P}{2\pi E}\left[(1+v)z^2(r^2+z^2)^{-3/2} + 2(1-v^2)(r^2+z^2)^{-1/2}\right] \tag{8}$$

where E and v are the modulus of elasticity and Poisson's ratio of the semi-infinite body respectively.
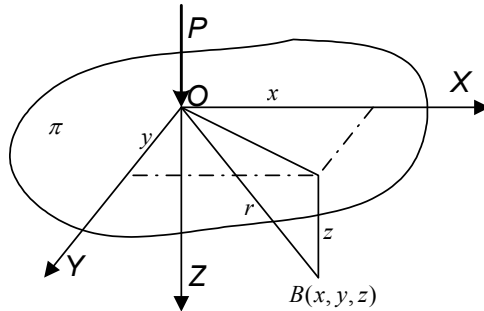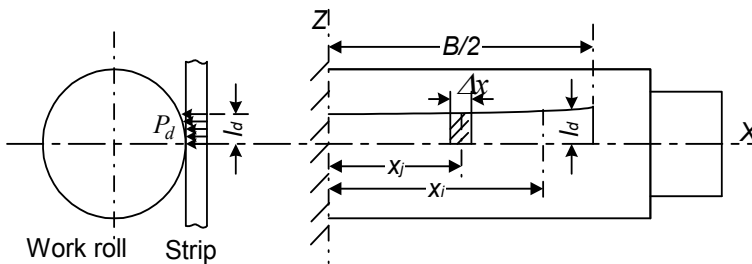
Fig. 3. Semi-infinite body model

Fig. 4. Flattening between the work roll and strip

Given in Fig. 4, the projected arc of contact between the work roll and strip, l_d, is not a constant and changes along the strip width that can be deduced by Hitchcock model (Wang, 1986)

$$l_d = \sqrt{R_w\left(\Delta h_i + \frac{16p_i}{\Delta x_i}\left(\frac{1-v_w^2}{\pi E_w}\right)\right)} \tag{9}$$

where Δh_i is the absolute reduction at element i, R_w is the radius of the work roll. Due to the maximum value of l_d is far less than the work roll diameter, so the work roll can be approximatively treated as a semi-infinite body. The influence function for the flattening between the work roll and the strip was derived according to a semi-infinite body model (Wang, 1986). However, the roll is not a real semi-infinite body, a modified model and the flattening between the work roll and strip can be calculated by

$$y_{ws}(i) = \sum_{j}^{n} g_{ws}(i,j)p_j \tag{10}$$

where y_{ws} is the flattening between the work roll and strip, the influence function for the flattening between the work roll and strip can be written as

$$g_{ws}(i,j) = \Phi\left(\left|x_i - x_j\right|\right) + \Phi\left(\left|x_i + x_j\right|\right) \tag{11}$$

where $\Phi(x)$ can be written as Eq. (12).

$$
\begin{aligned}
\Phi(x) = \frac{1-\nu_w{}^2}{E_w \pi \Delta x} \Bigg\{ &\ln \frac{\sqrt{l_d{}^2 + (x+\Delta x/2)^2} + x + \Delta x/2}{\sqrt{l_d{}^2 + (x-\Delta x/2)^2} + x - \Delta x/2} \\
&+ \frac{x+\Delta x/2}{l_d} \ln \frac{\sqrt{l_d{}^2 + (x+\Delta x/2)^2} + l_d{}^2}{|x+\Delta x/2|} \\
&- \frac{x-\Delta x/2}{l_d} \ln \frac{\sqrt{l_d{}^2 + (x-\Delta x/2)^2} + l_d{}^2}{|x-\Delta x/2|} \\
&- \frac{1}{2(1-\nu_w)} \Bigg[\frac{x+\Delta x/2}{\sqrt{R_w{}^2 + (x+\Delta x/2)^2}} - \frac{x-\Delta x/2}{\sqrt{R_w{}^2 + (x-\Delta x/2)^2}} \Bigg] \\
&- \ln \frac{\sqrt{R_w{}^2 + (x-\Delta x/2)^2} - (x-\Delta x/2)}{\sqrt{R_w{}^2 + (x+\Delta x/2)^2} - (x+\Delta x/2)} \Bigg\}
\end{aligned}
\tag{12}
$$

2.4 Flattening between the backup roll and work roll

Fig. 5 shows the flattening between the backup roll and work roll. It can also be found from Foppl model (Ginzburg & Azzam, 1997) that the flattening contact width between the backup roll and work roll is far less than the diameters of the work roll and backup roll, and it is suitable to calculate the flattening according to a semi infinite body model (Wang, 1986).
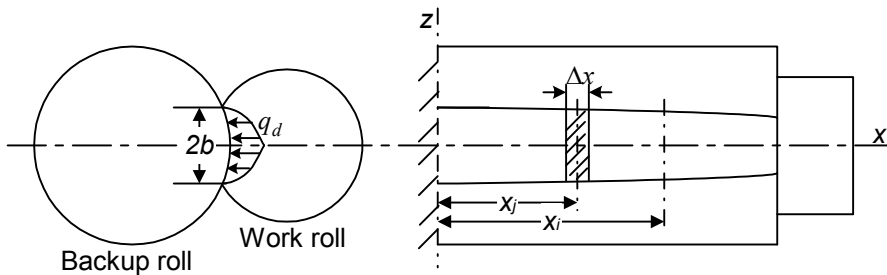

Fig. 5. Flattening between the backup roll and work roll

Assuming the contact pressure between the backup roll and work roll, q_d, is a parabolic distribution along the flattening contact width, $2b$ (see Fig. 6). As the backup roll and work roll are flattened at the same time, the flattening between the backup roll and work roll can be expressed as

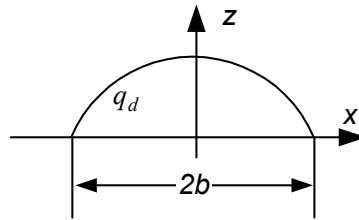$$y_{wb}(i) = \sum_{j}^{m} g_{wb}(i,j) q_j \tag{13}$$

Fig. 6. Distribution of contact pressure along the contact width

where y_{wb} is the flattening between the work roll and backup roll, the influence function is given

$$g_{wb}(i,j) = F_w\left(\left|x_i - x_j\right|\right) + F_w\left(\left|x_i + x_j\right|\right) + F_b\left(\left|x_i - x_j\right|\right) + F_b\left(\left|x_i + x_j\right|\right) \tag{14}$$

where $F(x)$ is a complex function derived by Wang (1986). $F_w(x)$ and $F_b(x)$ can be obtained when the corresponding values for the work roll and backup roll parameters respectively are introduced in Eq. (15).

$$
\begin{aligned}
F(x) = \frac{1-\nu^2}{E\pi\Delta x}\Bigg\{ & \frac{3}{4b}\Bigg[2b\ln\frac{\sqrt{b^2+(x+\Delta x/2)^2}+x+\Delta x/2}{\sqrt{b^2+(x-\Delta x/2)^2}+x-\Delta x/2} + 2(x+\Delta x/2)\ln\frac{\sqrt{b^2+(x+\Delta x/2)^2}+b}{|x+\Delta x/2|} \\
& -2(x-\Delta x/2)\ln\frac{\sqrt{b^2+(x-\Delta x/2)^2}+b}{|x-\Delta x/2|} + \frac{1}{3b}(x-\Delta x/2)\sqrt{b^2+(x-\Delta x/2)^2} \\
& -\frac{1}{3b}(x+\Delta x/2)\sqrt{b^2+(x+\Delta x/2)^2} - \frac{2}{3}b\ln\frac{\sqrt{b^2+(x-\Delta x/2)^2}-(x-\Delta x/2)}{\sqrt{b^2+(x+\Delta x/2)^2}-(x+\Delta x/2)} \\
& +\frac{1}{6b^2}(x+\Delta x/2)^3\ln\frac{\sqrt{b^2+(x+\Delta x/2)^2}+b}{\sqrt{b^2+(x+\Delta x/2)^2}-b} - \frac{1}{6b^2}(x-\Delta x/2)^3\ln\frac{\sqrt{b^2+(x-\Delta x/2)^2}+b}{\sqrt{b^2+(x-\Delta x/2)^2}-b}\Bigg] \\
& -\frac{1}{2(1-\nu)}\Bigg[\frac{x+\Delta x/2}{\sqrt{R^2+(x+\Delta x/2)^2}} - \frac{x-\Delta x/2}{\sqrt{R^2+(x-\Delta x/2)^2}}\Bigg] - \ln\frac{\sqrt{R^2+(x-\Delta x/2)^2}-(x-\Delta x/2)}{\sqrt{R^2+(x+\Delta x/2)^2}-(x+\Delta x/2)}\Bigg\}
\end{aligned}
\tag{15}
$$

2.5 Flattening between the upper and down work rolls

The work roll contacts at the edges outside the strip width are considered here as a new analysis of the cold rolling of thin strip. As shown in Fig. 7, the contact length between the upper and down work rolls due to strip plastic deformation, L_e, is far less than the length of roll barrel, it is not suitable for calculation by a semi-infinite body model. In the mean time, it is difficult to satisfy the accuracy during the iterative loop by using a semi-infinite body model due to few elements touching at the edges of the work rolls. Based on the study of

Wang (1983), when the modulus of the elasticity of the upper work roll is equal to that of the down work roll, i. e. $E_{wu} = E_{wl} = E$, the flattening between a pair of work rolls can be given directly by

$$y_{ww}(k) = \frac{2q_{ek}(1 - v_w^2)}{\pi E_w}\left(\frac{2}{3} + \ln\frac{2R_{wu}}{b} + \ln\frac{2R_{wl}}{b}\right) \tag{16}$$

where R_{wu} and R_{wl} are the radii of the upper and down work rolls respectively, b is a half of flattened contact width between the upper and down work rolls, which is given by

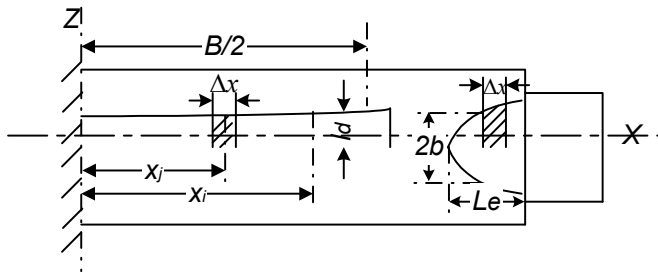$$b(k) = \sqrt{\frac{8(1 - v_w^2)q_{ek}}{\pi E_w}\frac{R_{wu}R_{wl}}{(R_{wu} + R_{wl})}} \tag{17}$$

Fig. 7. Flattening between the upper and down work rolls

2.6 Contour of compatibility
Under a rolling load, the deformation of the work roll, backup roll and the strip are described in Fig 8. Compatibility for the contact of the work roll and backup roll varies with the sum of the contour of the deformed work roll and backup roll, and the local flattening of the rolls. It can be calculated by the relationship

$$y_{wb}(i) = y_{wb}(0) + y_b(i) - y_w(i) - m_b(i) - m_w(i) \tag{18}$$

where $y_{wb}(0)$ is the centreline value of flattening between the work roll and backup roll, $m_b(i)$ and $m_w(i)$ are the combined machined and thermal cambers of the backup roll and work roll at element i respectively, m_b and m_w are the combined machined and thermal cambers of the backup roll and work roll at the centre of the roll barrel respectively.

The contour of the work roll surface in contact with the strip is determined by the combined influence of the rolling load, machined and thermal crown and the local flattening between the work roll and strip. The exit thickness of the strip at any point is the same as the loaded gap height at that point. Thus, the compatibility for contact of the work roll and strip can be expressed as

$$h(i) = h(0) + 2 \cdot (y_{ws}(i) - y_{ws}(0)) + 2 \cdot (m_w(i) - y_w(i)) \tag{19}$$

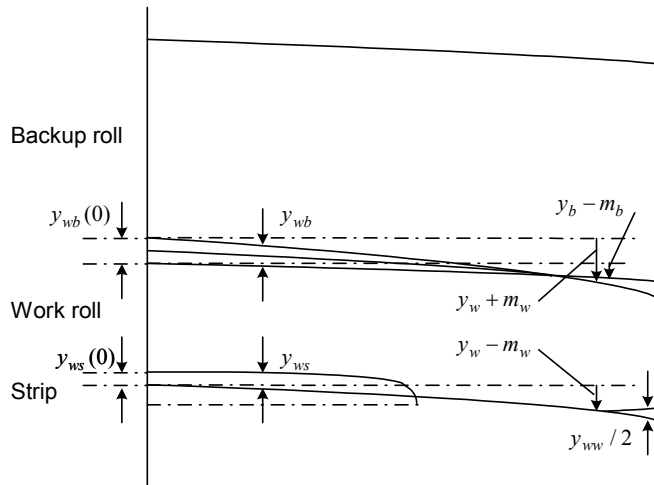where $y_{ws}(0)$ is the centreline value of flattening between the work roll and strip.

Fig. 8. Compatibility for contact of the work roll and backup roll, the work roll and strip, the upper and down work rolls

In the rolling of thin strip, the sides of work rolls beyond the strip width may touch and deform. The edge contacts between the upper and down work rolls affect the deformation of the roll and the strip. The compatibility for edge contact of the upper and down work rolls is calculated from the deformed work roll profile and the centreline value of the flattening between the work roll and strip, which is written as Eq. (20).

$$y_{ww}(i) = 2 \cdot y_{ws}(0) - h(0) + 2 \cdot (y_w(i) - m_w(i)) \tag{20}$$

2.7 Static equilibrium of work roll

Static equilibrium of the work roll is obtained by summing vertically the load between the work roll and backup roll, the load between the work roll and strip, the load between the upper and down work rolls, and the load applied to the work roll by the work roll bending mechanism. It can be expressed as Eq. (21).

$$\sum_{i=1}^{m} q_i - \sum_{i=1}^{n} p_i - \sum_{i=k}^{m} q_{ei} - F / 2 = 0 \tag{21}$$

2.8 Solution of equations

The iterative method was used to calculate the roll and strip deformation and the strip shape, as shown in Fig. 9.

3. Simulation conditions

The parameters used in the simulation for cold rolling of thin strip are as follows.

Work roll diameter: 63 mm	Work roll barrel: 249 mm
Work roll crown: 0 μm	Poisson's ratio of work roll: 0.3
Young's modulus of work roll: 22000 Kg/mm²	Distance between housing screw: 340 mm

Backup roll diameter: 228 mm

Backup roll barrel: 249 mm

Backup roll crown: 0 μm

Poisson's ratio of backup roll: 0.3

Young's modulus of backup roll: 22000 Kg/mm²

Slab thickness of strip: 0.5 mm

Central distance between bending cylinder: 340 mm

Entry thickness of strip: 0.30 mm

Exit thickness of strip: 0.10 mm

Width of strip: 140 mm

Back tension: 0 kN

Front tension: 0 kN

Rolling speed: 1 m/s

Initial crown of strip at entry: 0.0 mm

Friction coefficient: 0.1

Work roll bending force: 0 kN/chock

Defining point of strip crown from edge: 10 mm
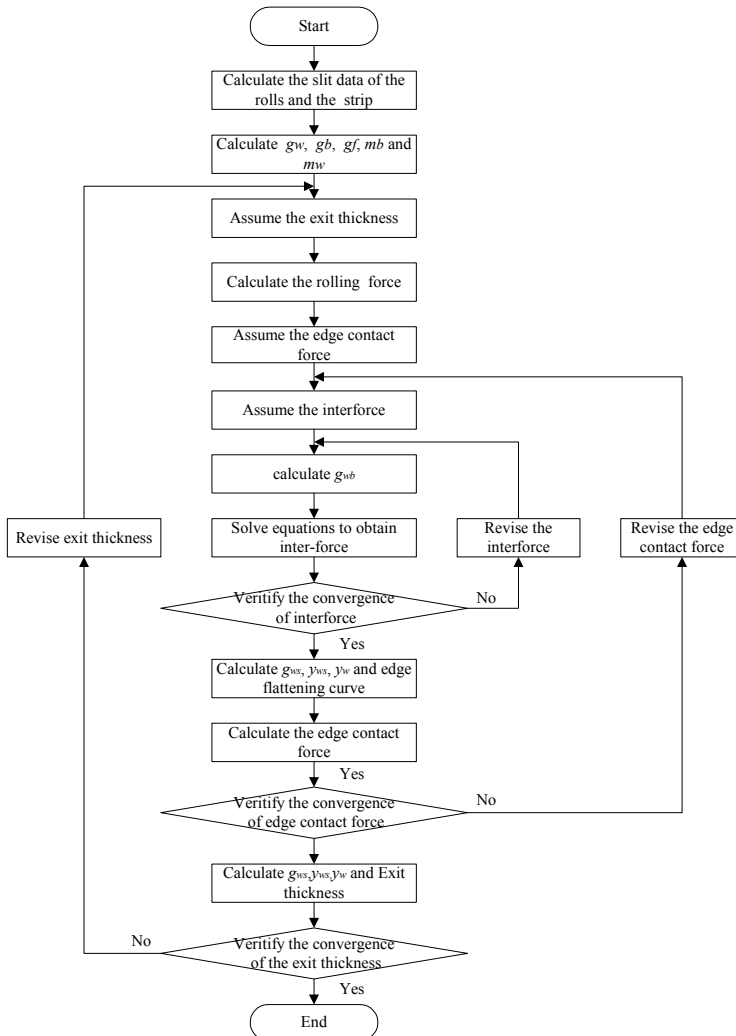
Fig. 9. Flow chart of the roll and strip deformation and strip shape calculation

Deformation resistance equation for strip is written as Eq. (22).

$$k_s = 740(\varepsilon_m + 0.01)^{0.23} \quad \text{(MPa)} \tag{22}$$

The slab thickness is 0.5 mm and the exit thickness of strip is 0.12 mm. The front and back tension is zero. The effects of the different rolling parameters such as the reduction, strip width, friction coefficient and the friction distribution along the strip width, on the mechanics and deformation of the cold rolling of thin strip are analyzed when an influence of edge contact force of the work rolls is considered. In the calculation, a significant concern is the rolling force, which is determined from the plasticity of the metal forming. The calculated rolling force is employed first, and then the further iterations are carried out.

For carbon steel rolling, the rolling force is calculated by using Bland-Ford-Hill model (Wang, 1983) considering the strip plastic deformation.

$$F = B \cdot k_p \cdot \sqrt{R'\Delta h} \cdot D_P \cdot \kappa \tag{23}$$

where κ is the tension factor, k_P is the dynamic deformation resistance which can be described by Eq. (24)

$$k_p = k_s \cdot (1000 \cdot \dot{\varepsilon})^{\alpha} \tag{24}$$

where α is a constant, $\dot{\varepsilon}$ is the stain rate and

$$k_s = k_0 \cdot (\varepsilon_m + m_1)^{n_1} \tag{25}$$

where k_0 is a constant, in this simulation $k_0 = 740$ MPa, m_1 and n_1 are constant, $m_1 = 0.01$ and $n_1 = 0.23$, ε_m is an average integral reduction which can be described as

$$\varepsilon_m = \ln\frac{H_1}{h_m} \tag{26}$$

where H_1 is slab thickness and

$$h_m = (1-\beta) \cdot H + \beta \cdot h \tag{27}$$

where β is a constant (0.75). R' is the flatten radius of work roll which can be deduced by Hitchcock model

$$R' = R \cdot \left\{1 + \frac{C_H \cdot P}{B \cdot (H-h)}\right\} \tag{28}$$

where H and h are the entry and exit thickness of strip, respectively, C_H is Hitchcock coefficient (Wang, 1983). D_P can be described as

$$D_P = 1.08 + 1.79\varepsilon\, f\sqrt{R'/H} - 1.02\varepsilon \tag{29}$$

where ε is the reduction and f the friction coefficient.

4. Results and discussion

4.1 Effect of edge contact on specific forces and strip profile

When the entry and exit thickness of strip is 0.2 mm and 0.12 mm respectively, friction coefficient 0.1, strip width 160 mm and the work roll bending force is zero. The calculated results such as the exit thickness distribution of strip along the strip width and the specific force distribution between the work roll and backup roll, between the upper and down work rolls, between the work roll and strip along the roll barrel with or without edge contact of the work rolls are shown in Fig. 10 and Table 1. It can be seen that the intermediate force closer to the edge of the roll barrel increases and the rolling force close to the side of the strip reduces due to the work roll edge contact. The maximum edge contact force at the edge of the roll barrel is larger than the backup work roll intermediate force, which will result in further wear of work rolls at this zone. The edge contact force between the upper and down work rolls is nearly 11 % of the rolling force. Due to the effect of the edge contact force of the work rolls, the crown of the strip reduces from 45.56 to 36.54 μm, and the edge contact of the work rolls can improve the strip shape when there is no work roll bending force applied. When the cold thin strip is rolled, the edge contact effect may occur and its effect must be introduced for calculating the roll and strip deformation, strip shape, thus forming a new analysis feature of the rolling process.

Status	Rolling force (kN)	Intermediate force (kN)	Edge contact force (kN)	Crown of exit strip (μm)	Edge contact length (mm)
Edge contact	595.99	661.29	65.30	36.54	36.0
No edge contact	620.25	620.25	0	45.56	0

Table 1. Comparison of specific forces and strip crown with or without edge contact effect
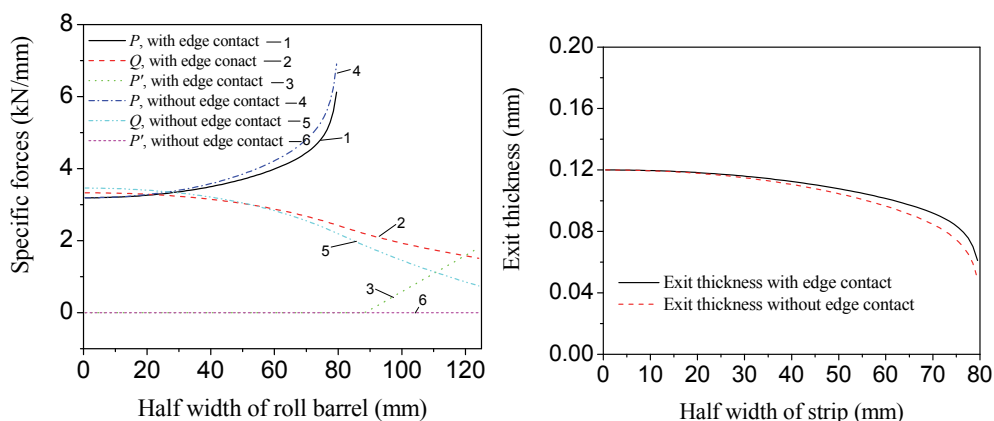

Fig. 10. Comparison of specific forces and exit thickness distribution with or without edge contact effect

4.2 Effect of reduction on forces and strip profiles

When the exit thickness of strip is 0.12 mm, friction coefficient 0.1, strip width 160 mm and no work roll bending force is applied, the entry thickness of the strip are 0.15, 0.17 and 0.2 mm respectively. The effect of the reduction on the specific forces (rolling force, intermediate force and edge contact force) and the exit thickness distribution is shown in Fig. 11 and Table 2. It can be seen that with increasing entry thickness of strip, the rolling force and intermediate force increase significantly, and at the same time the edge contact force and edge contact length of the work rolls have a tendency to increase, which are caused by an increase of reduction. It can also be seen that the strip profile (strip crown) reduces significantly when the reduction decreases (see Table 2). In the simulation, it is found that when the entry thickness is less than 0.1425 mm, which indicates that the reduction is less than 15.8 %, the upper and down work rolls do not touch and the edge contact force is zero. Therefore, under a certain exit thickness of strip, the strip shape and profile become poor with an increase of the reduction although there is a tendency of an increase of the edge contact forces.
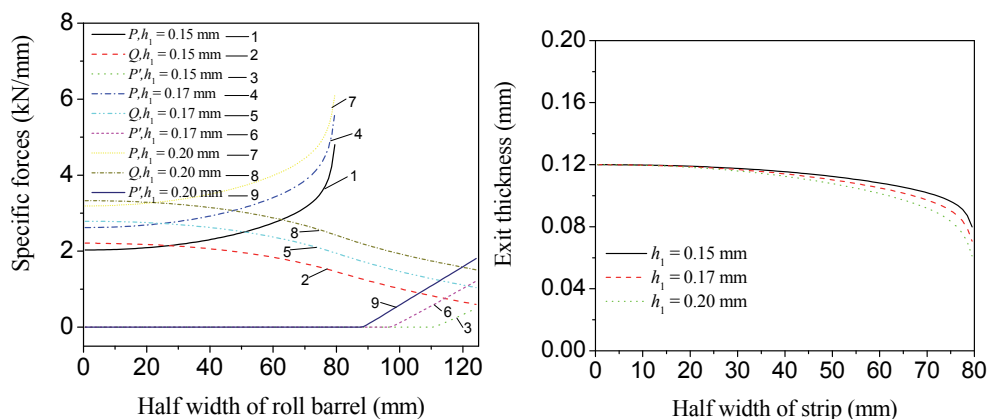

Fig. 11. Effect of entry thickness on specific force and exit thickness distribution

Entry thickness (mm)	Rolling force (kN)	Intermediate force (kN)	Crown of exit strip (μm)	Edge contact force (kN)	Edge contact length (mm)
0.15	401.30	408.09	23.62	6.79	13.0
0.17	504.11	536.81	29.67	32.69	27.0
0.20	595.99	661.29	36.54	65.30	36.0

Table 2. Comparison of specific forces and strip profiles for different entry thickness

4.3 Effect of strip widths on simulation results

The effect of the strip widths on the work roll edge contact force is more complex. In the calculation, the strip entry and exit thickness are 0.17 mm and 0.12 mm respectively, the

friction coefficient is 0.1 and the work roll bending force is zero. The strip widths of 80, 100, 120, 140, 160 and 180 mm were introduced in the analysis. The effect of the strip widths on the exit strip thickness distribution is shown in Fig. 12. It can be seen that with a narrower strip, the strip shape and profile are improved and the rolling force, intermediate force and edge contact force also reduce significantly (see Table 3). If the strip width is larger and more close to the edge of the rolls, the deflection of the work roll increases by a combined effect of the change of the distribution of the rolling force and intermediate force when the strip widths vary (see Fig. 13a and b), so the edge contact force and contact length of the work rolls increase accordingly, as shown in Fig. 13c. If the strip widths are less than 100 mm, the deflection of the work roll at the edge and the edge contact force will reduce with a narrower strip. It can be concluded that the strip width has a significant influence on the edge contact force and edge contact length of work rolls, which can result in an unstable work roll edge wear.

4.4 Effect of friction on calculation results

The lubrication and friction of the strip is a key issue in cold rolling process. The values of the friction coefficient may change significantly in different cold rolling mills and different operating conditions. The effects of the different friction coefficients on the edge contact of the work rolls are shown in Table 4 and Fig. 14. The entry and exit thickness of strip are 0.17 and 0.12 mm respectively, the strip width is 160 mm, and no work roll bending force is applied. With an increase of friction coefficient, the rolling force, intermediate force and edge contact force of the work rolls increase significantly. On the other hand, the strip shape reduces to 25.91 μm from 31.61 μm when the friction coefficient increases from 0.07 to 0.13. Although a higher rolling force has a tendency to make the strip shape poorer, the increase of edge contact forces with friction coefficient has a major effect on the improvement of the strip profile. Therefore, when the friction coefficient increases, the edge contact force of the work rolls increases, which is helpful in improving the strip profile.

The friction coefficient along the strip width is not a constant due to the change along the strip width of operating parameters, i.e. the rolling force, reduction and rolling speed etc.
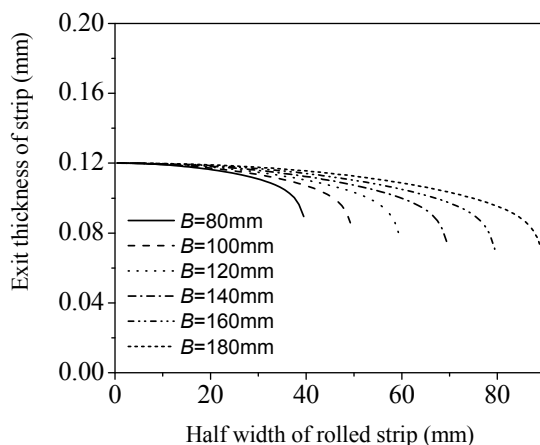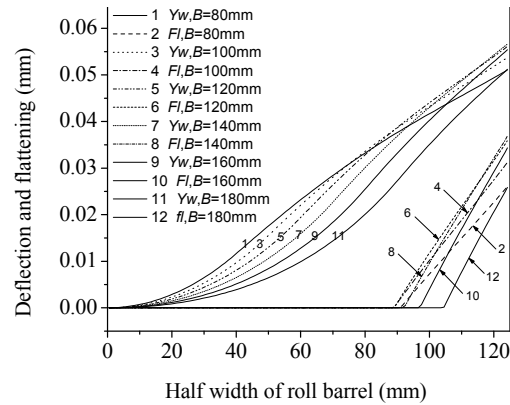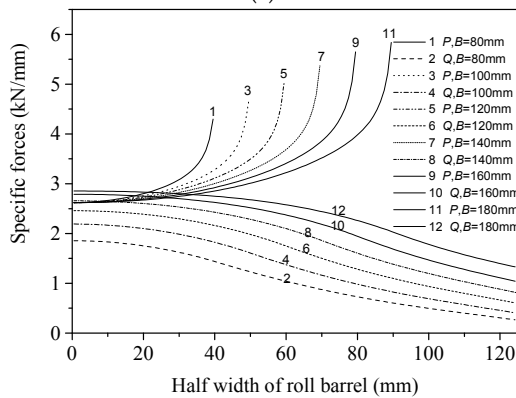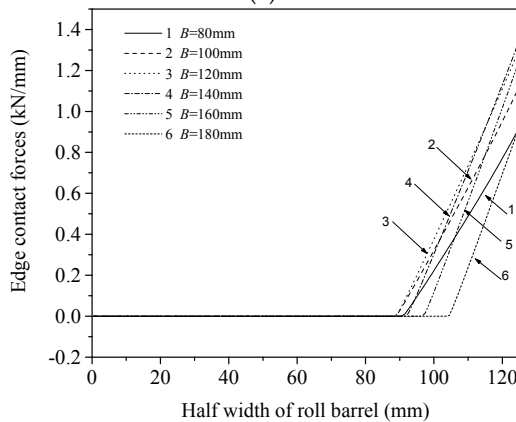

Fig. 12. Effect of the strip widths on the distribution of exit strip thickness

(a)

(b)

(c)

Fig. 13. Effect of the strip widths on the roll deflection and flattening (a), specific forces (b) and edge contact forces (c)

However, there are no reports on the effect of the friction variation along the strip width due to the complexity of this problem. In this section, the entry thickness of strip is 0.30 mm, exit thickness of strip 0.10 mm, strip width 140 mm, back tension 0 kN, front tension 0 kN, metal flow resistance is described by Eq. (22), and no work roll bending force is applied, and the different transverse friction coefficients were assumed to be constant f, parabolic increasing f_i and parabolic decreasing f_d along the strip width as shown in Fig. 15.

Width of strip (mm)	Rolling force (kN)	Intermediate Force (kN)	Crown of exit strip (μm)	Edge contact force (kN)	Edge contact length (mm)
80	235.39	264.05	14.48	28.66	33.0
100	300.27	337.74	18.78	37.48	35.0
120	367.83	411.52	23.05	43.68	35.0
140	435.91	478.38	26.70	42.47	32.0
160	504.11	536.81	29.67	32.69	27.0
180	569.96	587.76	31.65	17.80	20.0

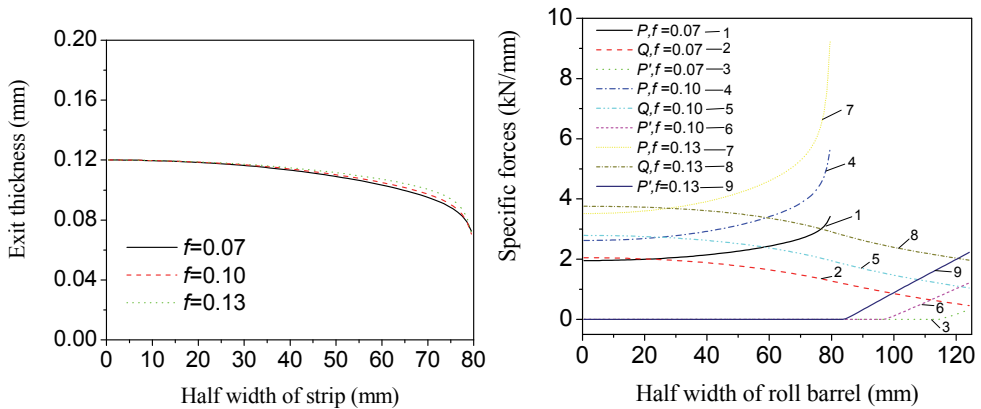Table 3. Comparison of specific forces and strip crowns with different strip widths

Fig. 14. Effect of friction coefficient on exit thickness distribution and specific forces

Friction coefficient	Rolling force (kN)	Intermediate force (kN)	Crown of exit strip (μm)	Edge contact force (kN)	Edge contact length (mm)
0.07	362.04	365.20	31.61	3.17	9.0
0.10	504.11	536.81	29.67	32.69	27.0
0.13	686.28	776.22	25.91	89.94	40.0

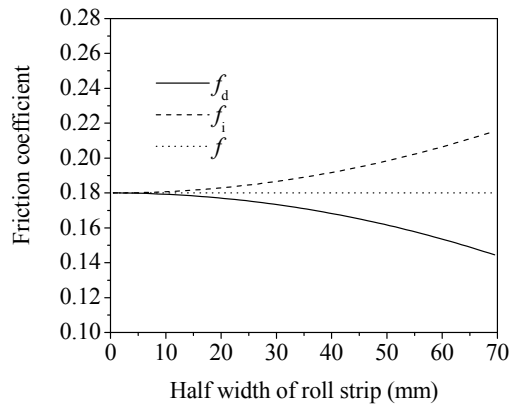Table 4. Comparison of specific forces and strip crowns with different friction coefficients

Fig. 15. Distribution of friction coefficient along the strip width

The effects of the transverse friction on the strip profile and specific forces i.e. the rolling force, intermediate force and edge contact force are shown in Figs. 16 and 17. It can be seen that the transverse friction has a significant effect on the strip profile. As the friction coefficient at the edge of strip increases, the exit crown of strip reduces, which indicates that the strip shape becomes better. Thus the strip shape and profile of thin strip can be improved by increasing the edge friction along the strip width. It can also be seen that the rolling force P increases significantly with the friction coefficient at the edges of strip. The intermediate force Q and edge contact force P' increase substantially with a higher friction coefficient at the edge of strip, and the length of edge contact also increases. Therefore, the length of edge contact can be determined from this developed model, which is helpful in understanding the feature of the thin strip rolling with work roll edge contact.
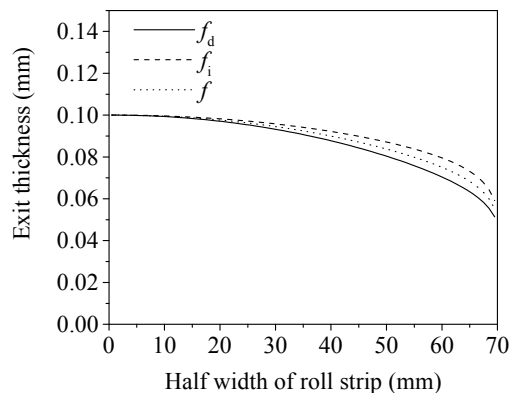

Fig. 16. Effect of transverse friction on strip shape

In order to verify the simulation results, the clod rolling of thin strip was conducted in lab. When the rolling speed is 0.27 m/s, entry thickness of strip is 0.55 mm, exit thickness 0.12 - 0.17 mm, strip widths 100 - 160 mm, a low carbon steel was rolled on Hille 100 rolling mill, friction coefficient is 0.1, its deformation resistance as described in Eq. (30) replaces Eq. (22) in the simulation.
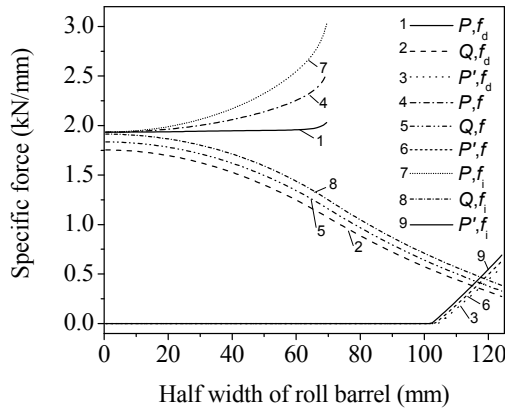
Fig. 17. Effect of transverse friction on specific forces

$$k = 403.53 \cdot \left(\varepsilon_m - 0.0067\right)^{0.1271} \times (1000\dot{\varepsilon})^{0.0123} \qquad (30)$$

Other rolling mill parameters are the same as above. Comparison of the calculated rolling forces with the measured values for various strip widths is shown in Fig. 18. It can be seen that the calculated rolling force increases with the strip width, and it is in good agreement with the measured value. Fig. 19 shows a comparison of the measured rolling force with the calculated rolling force under various strip widths and rolling speeds. It can be seen that the rolling force decreases significantly with an increase of the rolling speed. The variation of interference friction features between the roll and strip under various rolling speeds is the main reason for this result. The calculated rolling force is in good agreement with the measured value, which verifies the plastic deformation model we have developed for this thin strip rolling. At lower rolling speeds, the work roll edge contact force becomes higher.
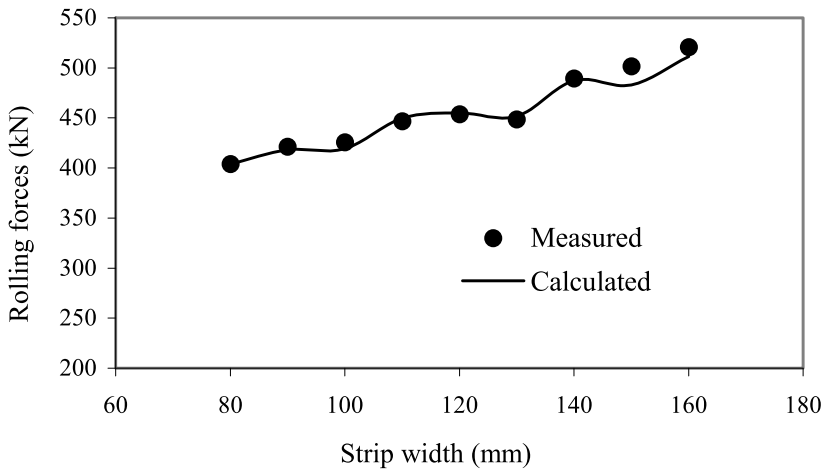

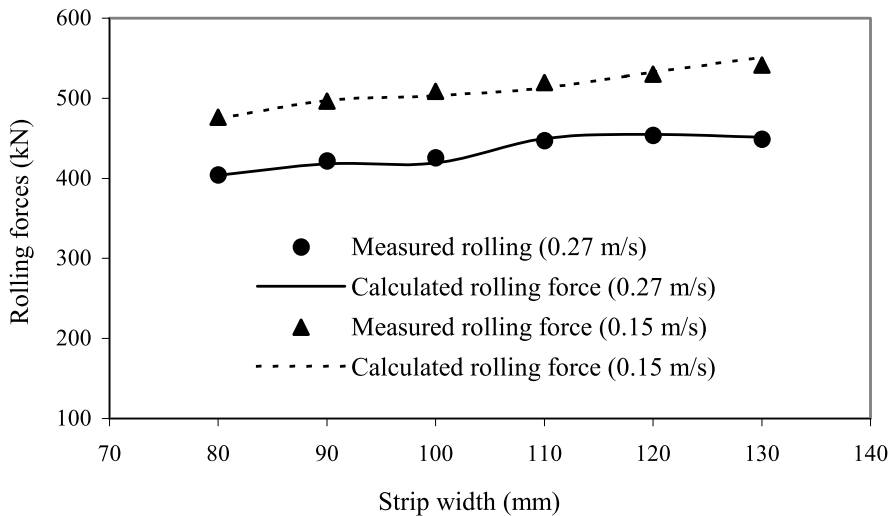Fig. 18. Comparison of the calculated rolling forces with the measured values

Fig. 19. Effects of the rolling speeds and strip widths on rolling forces

The average percentages of work roll edge contact force with respect to the total rolling force for various strip widths are 15.0 and 15.6 % for rolling speeds of 0.27 and 0.15 m/s, respectively. Therefore, the work roll edge contact force plays an important role in this rolling process.

5. Conclusions

A new model for rolling mechanics of thin strip in cold rolling has been developed successfully when the work rolls edge contacts. A strip plastic deformation-based model of the rolling force was employed in the calculation, and a modified semi-infinite body model was introduced to calculate the flattening between the work roll and backup roll, and the flattening between the work roll and strip, as well as a Foppl model was employed to calculate the edge contact between the upper and down work rolls. Based on the theory of the slit beam, the special rolling and strip deformation was simulated using a modified influence function method.

The calculated results show that the specific forces such as the rolling force, intermediate force and the shape and profile of the strip for this special rolling process are significantly different from the forces in the traditional cold rolling process, and those form a new theory of metal plasticity in metal rolling. The edge contact of the work rolls can improve the strip shape when no work roll bending force is applied. With an increase of reduction, the rolling force, intermediate force and edge contact force increase significantly, however the strip shape becomes poor. Strip width has a significant influence on the edge contact force and edge contact length of the work rolls, which can result in an unstable work roll edge wear. When the friction coefficient increases, the edge contact force between the two work rolls increases, this can improve the strip profile. The transverse friction has a significant effect on the rolling force, edge contact force and the length of edge contact. It affects the strip shape

and profile significantly, which is helpful in improving the strip shape and profile by modifying transverse friction. The calculated rolling force increases when the strip width increases and the rolling speed decreases, and it is in good agreement with the measured value. At lower rolling speeds, the work roll edge contact force becomes higher as a percentage of the total rolling force.

6. Nomenclature

b	A half of flattened contact width between the upper and down work rolls
B	Width of strip
D_w	Diameter of the work roll
D_b	Diameter of the backup roll
d_w	Diameter of the work roll neck
d_b	Diameter of the backup roll neck
E_w , E_b	Young's modulus of the work roll and backup roll respectively
fl	Roll flattening
F	Bending force
f	Friction coefficient
H_1	Slab thickness
H	Entry thickness of strip
h	Exit thickness of strip
I_b	Moment of inertia of the backup roll section
I_w	Moment of inertia of the work roll section
l_d	Projected arc of contact between the work roll and strip
k_0	Constant
k_p	Dynamic deformation resistance
k_s	Static deformation resistance
L_w	Width of the work roll barrel
L_b	Width of the backup roll barrel
L_1	Central distance between the work roll bending cylinders
L_2	Central distance between the housing screws
L_e	Edge contact length between the upper and down work rolls
m	Slab number of half of the roll barrel
m_1	Constant
m_w , m_b	Combined machined and thermal cambers of the work roll and backup roll at the centre of the roll barrel respectively
n	Slab number of half of the strip
n_1	Constant
P	Rolling force
q_j	Intermediate force between the work roll and backup roll at element j
p_j	Rolling force at element j
q_{em}	Edge contact force between the upper and lower works at element m
$R^{'}$	Flatten radius of work roll
R_{wu}	Radius of the upper work roll

|	
R_{wl}	Radius of the down work roll
y_w	Vertical deflection of the work roll
y_b	Vertical deflection of the backup roll
y_{ws}	Flattening between the work roll and strip
y_{wb}	Flattening between the work roll and backup roll
y_{ww}	Flattening between the upper and down work rolls
$y_{wb}(0)$	Centreline value of flattening between the work roll and backup roll
$y_{ws}(0)$	Centreline value of flattening between the work roll and strip
Yw	Roll deflection
Δh_i	Absolute reduction at element i
Δx	Width of each element
v_w , v_b	Poisson's ratio of the work roll and backup roll respectively
ε	Reduction
ε_m	Average integral reduction
$\dot{\varepsilon}$	Strain rate
β	Constant

7. Acknowledgements

8. References

Buchheit, T.E., Wellman, G.W., Battaile, C.C., 2005. Investigating the limits of polycrystal plasticity modeling. Int. J. Plas. 21(2), 221-249.

Edwards, W.J., Spooner, P.D., 1973. Analysis of strip shape. In: Bryand, G.F. (ed), Automation of Tandem Mills. Iron and Steel Institute, London, p. 177-212.

Ginzburg, V.B., 1989. Steel-rolling technology: theory and practice. Marcel Dekker Inc., New York, pp. 730-748.

Ginzburg, V.B., Azzam, M., 1997. Selection of optimum strip profile and flatness technology for rolling mills. Iron & Steel Engineer 74(7), 30-38.

Han, C.-S., Wagner, R.H., Barlat, F., 2004. On precipitate induced hardening in crystal plasticity: algorithms and simulations. Int. J. Plas. 20(8-9), 1441-1461.

Ho, K.C., Lin, J., Dean, T.A., 2004. Modelling of springback in creep forming thick aluminum sheets. Int. J. Plas. 20(4-5), 733-751.

Huh, M.Y., Lee, K.R., Engler, O., 2004. Evolution of texture and strain states in AA 3004 sheet during rolling with a dead block. Int. J. Plas. 20(7), 1183-1197.

Iwamoto, T., 2004. Multiscale computational simulation of deformation behavior of TRIP steel with growth of martensitic particles in unit cell by asymptotic homogenization method. Int. J. Plas. 20(4-5), 841-869.

Jiang, Z.Y., Tieu, A.K., 2001. A method to analyse the rolling of strip with ribs by 3-D rigid visco-plastic finite element method. J Mater. Process. Technol. 117(1-2), 146-152.

Jiang, Z.Y., Tieu, A.K., 2003a. Modelling of thin strip rolling with friction variation by a 3-D finite element method. JSME Int. 46(A3), 218-223.

Jiang, Z.Y., Tieu, A.K., Zhang, X.M., Lu, C., Sun, W.H., 2003b. Finite element simulation of cold rolling of thin strip. J Mater. Proc. Technol. 140(1-3), 544-549.

Jiang, Z.Y., Zhu, H.T., Tieu, A.K., 2003c. Effect of rolling parameters on cold rolling of thin strip during work roll edge contact. J Mater. Proc. Technol. 140(1-3), 537-543.

Kim, H.-K., Oh, S.-I., 2003. Finite element analysis of grain-by-grain deformation by crystal plasticity with couple stress. Int. J. Plas. 19(8), 1245-1270.

Komori, K., 1998. Analysis of cross and vertical buckling in sheet metal rolling. Int J Mech. Sci. 40(12), 1235-1246.

Kuhn, H.A., Weinstein, A.S. 1970, Lateral distribution of pressure in thin strip rolling. J Eng. for Industry, 453-460.

Le, H.R., Sutcliffe, M.P.F., 2001. A robust model for rolling of thin strip and foil. Int. J. Mech. Sci. 43, 1405-1419

Lenard, J.G., 1992. Friction and forward slip in cold strip rolling. Tribol. Trans. 35(3), 423-428.

Lenard, J.G., 1998. The effect of lubricant additives on the coefficient of friction in cold rolling. J Mater. Process. Technol. 80-81, 232-238.

Lin, Z-C., Lee, S-Y., 1997. An investigation of contact problem between strip and work roll with a smooth straight surface during cold rolling. Int J Mech. Sci. 39(12), 1385-1404.

Liu, Y.J., Tieu, A.K., Wang, D.D., Yuen, W.Y.D., 2001. Friction measurement in cold rolling. J Mater. Process. Technol. 111, 142-145.

Martin, P.H., Smith, L.M., 2005. Practical limitations to the influence of through-thickness normal stress on sheet metal formability. Int. J. Plas. 21(4), 671-690.

Shi, J., McElwain, D.L.S., Langlands, T.A.M., 2001. A comparison of methods to estimate the roll torque in thin strip rolling. Int. J. Mech. Sci. 43, 611-630.

Shohet, K.N., Townsend, N.A., 1968. Roll bending methods of crown control in four-high plate mill. J Iron and Steel Institute 11, 1088-1098.

Smith, L.M., Averill, R.C., Lucas, J.P., Stoughton, T.B., Matin, P.H., 2003. Influence of transverse stress normal stress on sheet metal formability. Int. J. Plas. 19(10), 1567-1583.

Stone, M.D., Gray, R., 1965. Theory and practice aspects in crown control. Iron Steel Eng. XLII(8), 73-83.

Stoughton, T.B., Yoon, J.-W., 2004. A pressure-sensitive yield criterion under a non-associated flow rule for sheet metal forming. Int. J. Plas. 20(4-5), 705-731.

Stupkiewicz, S., Mroz, Z., 2003. Phenomenological model of real contact area evolution with account for bulk plastic deformation in metal forming. Int. J. Plas. 19(3), 323-344.

Sutcliffe, M.P.F., Rayner, P.J., 1998. Experimental measurements of load and strip profile in thin strip rolling. Int. J. Mech. Sci. 40, 887-899.

Timoshenko, S.P., Goodier, J.N., 1970. Theory of elasticity. McGraw-Hill, Third edition, New York.

Wang, G.D., 1986. The shape control and theory. Metallurgical Industry Press, Beijing, pp. 225-379 (in Chinese).

Wang, T., 1983. Rolling technology. Metallurgical Industry Press, Beijing (in Chinese).
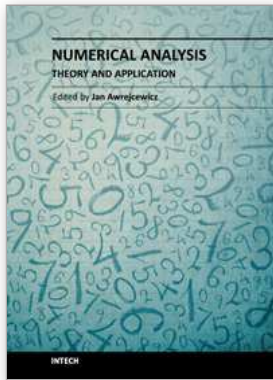
Numerical Analysis - Theory and Application

Edited by Prof. Jan Awrejcewicz

Numerical Analysis â€" Theory and Application is an edited book divided into two parts: Part I devoted to Theory, and Part II dealing with Application. The presented book is focused on introducing theoretical approaches of numerical analysis as well as applications of various numerical methods to either study or solving numerous theoretical and engineering problems. Since a large number of pure theoretical research is proposed as well as a large amount of applications oriented numerical simulation results are given, the book can be useful for both theoretical and applied research aimed on numerical simulations. In addition, in many cases the presented approaches can be applied directly either by theoreticians or engineers.

How to reference

In order to correctly reference this scholarly work, feel free to copy and paste the following:

INTECH
open science | open minds